Zoomorphology (2019) 138:419–424
https://doi.org/10.1007/s00435-019-00451-7

METHODS PAPERS

A farewell to arms: using X-ray synchrotron imaging to investigate autotomy in brittle stars

E. G. Clark[1] · K. Fezzaa[2] · J. E. Burke[1] · R. A. Racicot[3,4] · J. O. Shaw[1] · S. Westacott[1] · D. E. G. Briggs[1,5]

Received: 11 January 2019 / Revised: 15 May 2019 / Accepted: 27 May 2019 / Published online: 5 June 2019

Abstract

Autotomy, the self-induced loss of a body structure, occurs in every living class of echinoderms and is related to the remarkable regeneration capabilities of the group. It is particularly prevalent in brittle stars (Class Ophiuroidea). Autotomy is facilitated by mutable collagenous tissue, which undergoes nervous system-mediated changes in tensile stiffness, tensile strength, and viscosity. The previous investigations of autotomy have been based on observations of the external surface, surgical manipulation of internal structures, or data on the morphology of structures post-autotomy. We used fast phase-contrast X-ray synchrotron imaging to visualize full autotomy events in vivo in the arms of specimens of the brittle star *Ophioderma brevispina*. This method requires no chemical or surgical manipulation and enabled us to identify several key stages in the autotomy process. We used this methodology to observe critical changes within the internal structure of the arm as it transitions from a functional mechanical apparatus to a dysfunctional disarticulated state. This method is the first in which the full intersegmental plane of the arm can be observed during autotomy. It can be applied to visualize autotomy and motion in vivo in other brittle star taxa, as well as in other groups such as asteroids and arthropods.

Keywords Autotomy · Ophiuroidea · Mutable collagenous tissue · Synchrotron imaging

Introduction

Autotomy, the self-induced loss of a viable body structure mediated by the nervous system (Wilkie 2001), is a defensive process in which an organism strategically detaches part of its body in response to a perceived threat, often to avoid predation. This phenomenon has been observed in at least nine phyla (Wilkie 1978a, b; Fleming et al. 2007). Autotomy may also be integral to the regeneration process, as regeneration of structures from regions other than the autotomy plane may result in anomalies in taxa such as crinoids and decapod crustaceans (Wilkie 2001).

Autotomy is the most widespread cause of structural loss in echinoderms (Wilkie 2001). This process occurs in certain members of each extant echinoderm class, resulting in the loss of a range of structures in crinoids (arms, cirri, pinnules, and stalks), asteroids (arms), ophiuroids (arms, aboral disk comprising the stomach, gonads, and genital bursae), echinoids (globiferous pedicellariae), and holothurians (digestive tract, respiratory structures, haemal vessels, gonads, feeding tentacles, and the aquapharyngeal bulb) (Wilkie 2001). There is debate over the influence of autotomy versus other processes that result in structural loss affecting the crown and visceral mass in crinoids, the pedicells and papulae in asteroids, and the spines in asteroids, ophiuroids, and echinoids (Wilkie 2001).

As shown in a number of seminal papers by Wilkie (Wilkie 1978a, b, c, 2005; Wilkie and Emson 1987), echinoderm autotomy is facilitated by mutable collagenous tissue

Electronic supplementary material The online version of this article (https://doi.org/10.1007/s00435-019-00451-7) contains supplementary material, which is available to authorized users.

✉ E. G. Clark
elizabeth.g.clark@yale.edu

[1] Department of Geology and Geophysics, Yale University, New Haven, CT 06511, USA

[2] X-ray Science Division, Advanced Photon Source, Argonne National Laboratory, Lemont, IL 60439, USA

[3] Department of Earth and Environmental Science, Vanderbilt University, Nashville, TN 37240, USA

[4] W.M. Keck Science Department, Claremont McKenna, Pitzer, and Scripps Colleges, Claremont, CA 91711, USA

[5] Yale Peabody Museum of Natural History, Yale University, New Haven, CT 06511, USA

(MCT). MCT is a tissue type exclusive to echinoderms and found in all echinoderm groups (Wilkie 1984). MCT can undergo drastic nervous system-mediated loss of tensile strength in a second or less, and stiffen to maintain posture without expending any energy (Wilkie 1984). Research on MCT is being applied to advance pharmacology and material sciences (Wilkie 2005; Barbaglio et al. 2013; Ferrario et al. 2017; Goh and Holmes 2017).

Arm loss is commonly found in ophiuroids (brittle stars): in natural populations, up to 99% of brittle star arms have been observed to be actively regenerating (Wilkie 1978a). The segments of most brittle star arms comprise a large central ossicle (the "vertebra") surrounded by four smaller plates on its dorsal, ventral, and right and left lateral surfaces. Adjacent segments are connected by MCT, which makes up the tendons of the four intervertebral muscles, the intervertebral ligament, and the ligaments connecting the non-vertebral plates (Wilkie 1978b). The intervertebral areas of each ossicle, associated with the intervertebral ligament, meet to form an often complex interlocking interface known as the intervertebral joint (Clark et al. 2018a). The previous investigations have shown that autotomy does not exploit a weak area of the arm, but is the result of a change in the tensile strength of the otherwise robust tendons and ligaments (Wilkie 1978a). Ophiuroids have hundreds of potential autotomy planes, as they can shed a portion of the arm at the articulation between any two segments (Wilkie 2001).

Our current understanding of the structural changes and functional processes underlying ophiuroid arm autotomy are based on observations of external morphology (Wilkie 1978a, b), investigations of structures post-autotomy (Wilkie 1978b), and surgery or serial sectioning of autotomizing internal structures (Wilkie 1978a, c; Wilkie and Emson 1987). Autotomizing arms were embedded in plasticine to arrest and observe the arm at different stages of the process (Wilkie 1978a). Arm segments have been examined to visualize the external structure of the autotomy plane following autotomy (Wilkie 1978b; Wilkie and Emson 1987). In addition, several experiments have been conducted to investigate the physiology of the process (e.g., Wilkie 1978a, c; Wilkie and Emson 1987). A load was applied to partially dissected amputated arms to analyze the behavior of the connective tissue and the effect of various chemical pre-treatments (Wilkie 1978c). Autotomy was induced in partially dissected amputated arms to observe the behavior of the musculature (Wilkie and Emson 1987). Inducing autotomy in ophiuroids mounted with free-hanging arms demonstrated that external contact was not necessary for autotomy to occur (Wilkie 1978a). All of these techniques have revealed important aspects of this process, but they are all limited in one or more of the following ways: by relying on observations post-autotomy, revealing external anatomy only, not involving observations in vivo, or only showing a single stage of the process. Until now, it has not been possible to observe the sequence of events involved in autotomy directly nor to determine the role, if any, of adjacent segment connections.

We conducted fast phase-contrast edge-enhanced X-ray synchrotron radiographic imaging to stimulate autotomy and to image the autotomization process in live ophiuroids. Autotomy occurred as the animal attempted to shed the part of the arm being X-rayed. The method presented here is a new strategy for in vivo visualization. It is the only technique that reveals the autotomy process from start to finish in vivo, and allows the internal structure of the segments comprising the autotomy plane to be visualized throughout.

Materials and methods

We conducted live phase-contrast X-ray synchrotron imaging of brittle star skeletal tissue using beamline 32-ID at the Advanced Photon Source of Argonne National Laboratory (Westneat et al. 2003). 65 *O. brevispina* specimens were imaged individually. *O. brevispina* was selected due to its appropriate size and speed of movement for the imaging setup and parameters used. Specimens were mounted by surrounding the disk of the brittle star with cotton soaked in sea water. The disk was attached to a wooden craft stick with plastic cable ties. Arms were either free hanging or loosely constrained with cable ties to promote autotomy in a particular region. In several specimens, one arm was inserted into a small plastic tube (2–3 mm in diameter) which was glued to the end of the craft stick (Online Resource 1), and in several such specimens the arms that were not in the tube were removed, as extraneous arm movement entered the visual field and obscured the area of interest. The craft stick was oriented horizontally or vertically. The specific setup of each specimen is noted in "Results". The specimens were attached via the craft stick to a plastic clamp on a metal stand inside the experimental station of 32-ID-C beamline, with the oral/aboral axis oriented parallel to the beam. The metal stand was connected to a motorized stage which allowed the specimen to be positioned with the aid of a video camera so that the arm would be exposed to the beam and imaged simultaneously. A remotely operated mechanical shutter controlled the exposure to the X-ray beam. We used an X-ray energy of ~25 keV and a sample-detector distance of 25 cm. We imaged the specimens with 5× (2×) objectives with 2.25×1.41 (5.63×3.52) mm^2 field of view, and 1.17 (2.9) µm pixel size, respectively, at speeds between 30 and 87 frames per second. The actual point spread function (PSF) of the detection system was measured separately to be about 2.5 µm (with the 5× objective) using a knife-edge scan technique. The brittle star began autotomizing the arm at a position proximal to the beam (and, therefore, outside the imaging window) to try to shed the afflicted part. We moved

the specimen so that the autotomizing area was within the imaging window to capture the events. We took over one million images (1,227,728) of 65 specimens of *O. brevispina* over approximately 30 h; 1.4% of these images illustrate autotomy. We captured autotomy in one arm of each of four specimens and we observed changes in the properties of the MCT in several specimens differing from those observed in normal movement.

We did not capture autotomy in most of the specimens we imaged. Application of the beam generates this response only in a minority of cases (and never in a small subset that was submerged in water). Since autotomy tended to occur proximal to the beam application, several specimens autotomized outside the imaging window. Capturing autotomy involved moving the imaging window proximally within seconds of applying the beam and observing arm motion. We imaged specimens with different degrees of arm restriction (unrestricted, restricted with loose plastic cable ties, and confined within a narrow plastic tube). Some degree of arm restriction was essential for positioning the arm within the small imaging window, as the arm could move faster to escape the beam than the motors used to reposition the specimen. Restricting the arms also prevented movement of other arms from blocking the area of interest (as in specimen 2, see Online Resource 3). Maximum activity was ensured by minimizing the time between mounting and imaging the specimen. Trial and error determined that the mounting techniques presented here maximized the probability of observing autotomy.

Results

The beamline experimental parameters (beam energy, sample-detector distance, etc.) were set up so as to optimize the contrast and resolution. Most of the details on the collected images come from the skeleton rather than muscles and ligaments; hence, it was necessary to define autotomy in terms of the position of the ossicles. Autotomy was considered to have occurred when the morphology of the intervertebral area became irreversibly inviable for movement. During normal movement, pairs of the four intervertebral muscles contract and relax to move successive segments about the intervertebral joint (Clark et al. 2018a). Because *O. brevispina* has been observed to maintain articulations between successive vertebrae even as they approach their maximal range of motion (Clark et al. 2018a), separation between successive vertebrae at the intervertebral area is not a product of normal motion and involves changes in the tensile properties of the MCT. We defined movement as no longer viable when the point of rotation between two successive segments was no longer at the intervertebral joint (as in normal movement: Clark et al. 2018a), but had migrated laterally beyond the vertebrae to the lateral ossicles (Fig. 1c, g). In this configuration, both pairs of intervertebral muscles are extended, indicating that the intervertebral musculature no longer plays an effective role in arm motion. In two of the four specimens in which autotomy was captured, we observed several autotomizations in the same arm. In one specimen, the arm in which autotomy was imaged was positioned vertically in a tube (Specimen 1); in the other three, they were oriented horizontally and loosely constrained by cable ties (Specimens 2–4).

Specimen 1: This arm was constrained vertically within a tube. We imaged two autotomies and partial separation of seven intersegmental areas within sixteen segments (enumerated 1–16 distally to proximally). Segments 1 and 2 separated slightly with minimal movement in their vicinity, but accompanied by lateral undulation more proximally which resulted in an autotomy between segments 2 and 3. Lateral movement led to slight separation of segments 3 and 4. Flexure of the proximal portion of the arm to the right led to separation of segments 4 and 5 on that side. Flexure to the left then resulted in an autotomy between segments 5 and 6, which pivoted away from each other at the point of contact between the right laterals. Further movement to the right separated segments 6 and 7 and then 7 and 8. Subsequent motion to the left partially separated segments 11 and 12 and a quick thrash to the right autotomized 12 from 13, which pivoted away from one another at the point of contact of the left laterals (Fig. 1). Segments 15 and 16 appeared to separate partially and become rearticulated. Video of X-ray imaging data is presented in Online Resource 2.
Specimen 2: This arm was mounted horizontally on a craft stick and loosely constrained by a cable tie. The sample mounting process induced an autotomy in the distal region of the imaged arm. The proximal part of the arm made a swift vertical motion and released two segments at the remaining distal extremity. Those segments separated, as they pivoted away from each other at the point of contact between the left laterals (the view was partially obscured by motion of another arm). Video of X-ray imaging data is presented in Online Resource 3.
Specimen 3: This arm was mounted horizontally on a craft stick and loosely constrained by cable ties. The brittle star attempted to pull the arm out of the cable ties resulting in flexure of the proximal arm at about 45° to the disk and separation of segments at the maximum curvature. Two autotomies occurred in the proximal part of the arm as a result of the application of the beam in two separate places. In the first, the ossicles pivoted away from each other at the point of contact of the right laterals. Movement of the proximal arm to the left led to further separation. The second autotomy occurred between the

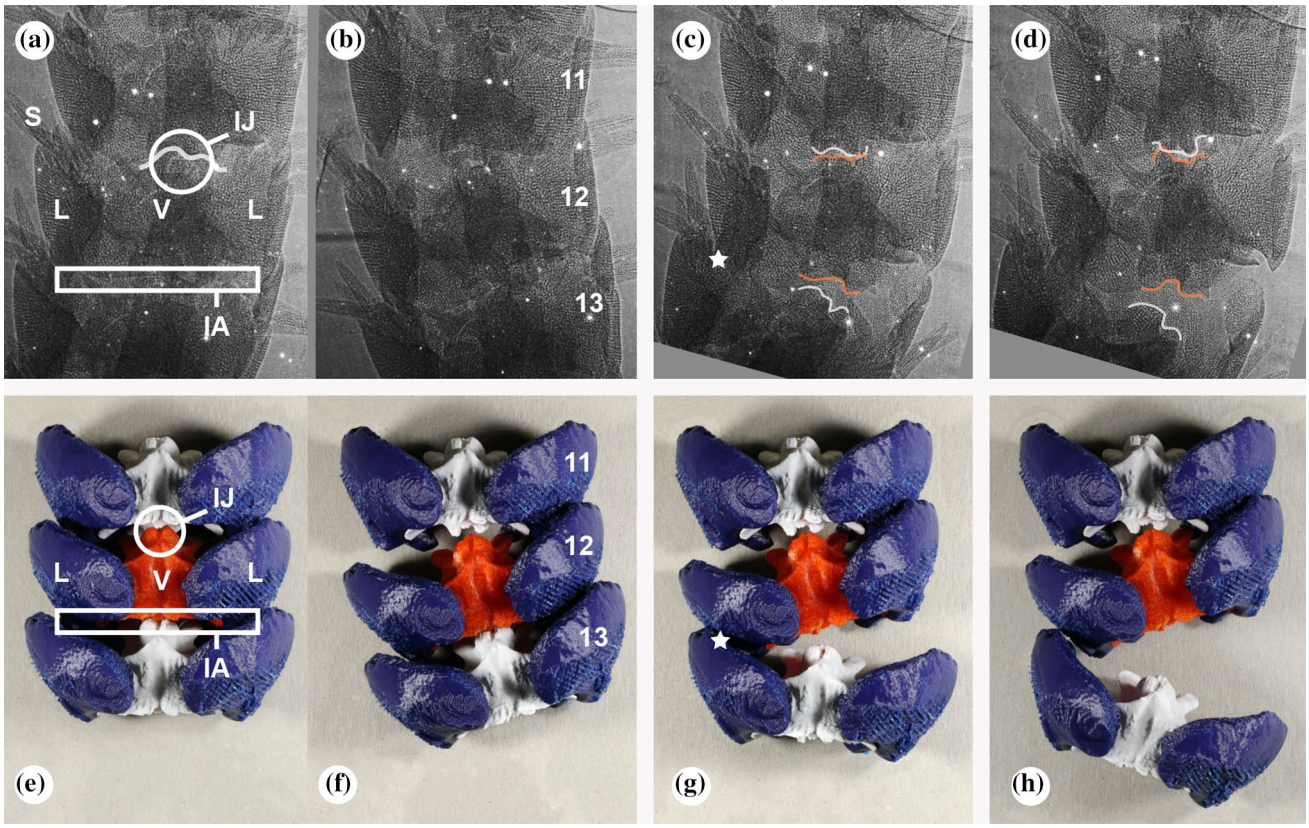

Fig. 1 **a**–**d** Radiograph projections of dorsal view of arm segments of Specimen 1 during autotomization. **e**–**h** 3D-printed models demonstrating the autotomy process. **a**, **e** Fully articulated arm. **b**, **f** Distal intersegmental area shows partial separation between segments 11 and 12. **c**, **g** Loss of tensile strength at autotomy plane and lateral undulation trigger autotomy between segments 12 and 13. Star indicates point of contact of the left laterals. **d**, **h** Additional separation between segments 12 and 13. *L* lateral ossicle, *V* vertebra, *IJ* intervertebral joint, *IA* intersegmental area, *S* spines. Segments numbered for descriptive purposes as in text. Width of segment in X-ray image is approximately 1 mm. Digital representations of the ossicles for the 3D prints were created by extracting watertight polygonal meshes from a micro-CT volume of *Ophioderma brevispina* (Clark et al. 2018a, b) as STL files. The STL files were imported into MakerBot Desktop (Brooklyn, NY), increased in size by 4000%, and printed using a MakerBot 3D 5th Generation Replicator

two segments proximal to the first one following several lateral undulations. Video of X-ray imaging data is presented in Online Resource 4.

Specimen 4: The junction between segments 1 and 2 (numbered from the attachment to the disk) was autotomizing at the start of imaging due to the application of the beam. A vertical undulation proximally, combined with the weight of the distal portion of the arm, pivoted segment 2 away from 3 at the contact of the left laterals, opening up the right side. Separation also occurred between segments 3 and 4. Subsequent downward motion of the arm juxtaposed segments 2, 3, and 4 in their original position. Video of X-ray imaging data is presented in Online Resource 5.

Observations of an additional arm in Specimen 4 and individual arms in three other specimens revealed a subtler separation of segments that suggest a change in the tensile properties of the MCT that did not accompany an autotomy (Online Resource 6–8). These included separation of successive ossicles at the intervertebral joint or partial separation at the joint interface due to excessive lateral flexion. In Specimen 5, the arm was positioned vertically in a tube. Separation of ossicles at an intervertebral joint was immediately followed by separation at the next proximal intervertebral joint. The intersegmental areas then rearticulated in the reverse order. Lateral undulation of proximal segments was tracked by similar movements distally (which does not occur in specimens which have undergone an autotomy or a complete loss of tensile stiffness of the MCT), suggesting that the MCT had returned to the original condition. Moving the specimen to image the more proximal part of the arm revealed additional separated segments that became rearticulated upon movement of this portion of the arm.

Discussion

The autotomization process represents the transition of sequential arm segments from a complex, articulated functional apparatus into a dissociated dysfunctional state. Our methodology allowed us to directly observe the morphological changes that occurred within the arm as it engaged in this transition. Despite variation in the mounting of specimens and the position of autotomies, two major events seem to be involved in the process of autotomization:

Step 1: Changes in tensile properties of the tissues at the autotomy plane. Loss of tensile strength and/or stiffness of the MCT in the autotomy plane was evidenced by the separation of vertebral ossicles of successive segments, which does not occur during normal arm movement (Clark et al. 2018a) (Fig. 1c).
Step 2: Application of force external to the autotomy plane. Lateral movements of the arm directly proximal to the autotomy plane facilitated the separation of the adjacent segments (Fig. 1c, d).

Step 1 occurred slightly before or synchronously with Step 2. Our observations confirm that the brittle star itself can induce autotomy, supporting the previous reports that emphasized the ability of the arm to autotomize in the absence of any external force or resistance (Wilkie 1978a, 1984, 1988, 2002). The separation of segments was facilitated by motion generated by the musculature of the proximal arm (Specimens 1–4), in some cases assisted by gravity (Specimens 2, 4) and external contact (Wilkie 1978b). In one case (Specimen 2), separation was facilitated by adhesion of two segments to the craft stick at a point distal to the autotomy plane. In nature, the force could be generated by a predator. In each autotomy event we observed, the lateral ossicles and spines of the proximal segment pressed against those distal to it during lateral flexion, opening the autotomy plane parallel to the force vector applied at the point of contact.

The autotomy events that we observed were all associated with either prior upstream autotomy events or separations between successive vertebrae within segments immediately distal to the autotomy planes. This may have been due to movement of the point where the beam was applied from the distal part of the arm proximally. However, a reduction in tensile stiffness upstream of the eventual autotomy plane would theoretically help facilitate autotomy: instead of moving the entire length of the arm, lateral flexion in the proximal portion would displace the segments only as far as the weak upstream zone. This lowers the effective mass of the displaced segment(s) which generate tensile strain on the MCT and facilitate separation. Thus, the formation of a weak upstream zone reduces the amount of energy required to cause autotomy. In this way, one autotomy would facilitate the occurrence of a second one more proximally. It is clear that changes in adjacent intersegmental areas may facilitate autotomization, even though they may not be evident on the external surface (Wilkie 1978a, b), but further work is needed to determine if this is the case or just a product of the methodology used here.

In several instances, a degree of separation at the intervertebral articulation evidenced a loss in tensile stiffness in the ligament but no autotomy occurred. Three states of variable tensility in MCT have been identified (Wilkie 2002): stiff, compliant, and friable. The compliant state functions in arm movement (Wilkie 2002). We observed a loss of tensile stiffness that was not associated with normal movement, but did not result in autotomy. This confirms Wilkie's (1988, 2002) observation that MCT can restiffen and need not proceed irreversibly to a friable state and rupture, and illustrates the potential of our method for investigating reversibility during the autotomy process. The rearticulation observed in specimens 1 and 5 may also reflect this process. Further exploration of the variable tensility and degree of reversibility during the stages of autotomy would be an interesting direction for future work. In addition, many specimens yielded images showing arm motion in vivo. Thus, this imaging method could be used to apply XROMM (Brainerd et al. 2010), a technique to visualize, model, and analyze motion that incorporates in vivo X-ray imaging data with 3D-digitized morphology, to the study of animals for which this methodology has not yet been used due to their small size.

Conclusion

Our experiments demonstrate the utility of rapid high-resolution X-ray imaging in investigating the steps underlying autotomy. The method allows changes within the ophiuroid arm, including reversals in the state of MCT, to be documented in vivo in real time. We consistently observed shifts in the tensile properties of the intersegmental MCT and the application of force by the animal external to the autotomy plane. There were indications of potential weakness in the MCT upstream of the eventual autotomy plane. Promising directions for further study of brittle star autotomy using the foundations of our methodology include assessing the presence of this weak upstream area, varying the imaging parameters to capture the changing properties of the soft tissues, and conducting comparative analyses of additional taxa. Rapid high-resolution X-ray imaging can also be applied to the study of brittle star arm mechanics as well as motion in other echinoderm groups. This imaging technique has the

potential to provide insights into autotomy and movement in other organisms such as asteroids and various arthropods (Fleming et al. 2007).

Acknowledgements We are grateful to Alex Deriy (Argonne National Labs), Pincelli Hull, Peter Williams (Yale University) and Carmen Soriano for assistance and valuable discussion. This research used resources of the Advanced Photon Source, a US Department of Energy (DOE) Office of Science User Facility operated for the DOE Office of Science by Argonne National Laboratory under Contract No. DE-AC02-06CH11357.

Author contributions EGC, KF, JEB, RAR, and JOS conducted the experiments. EGC, JEB, RAR, JOS, SW, and DEGB interpreted the results. EGC and DEGB prepared the manuscript with input from all authors.

Funding Funded by Yale University.

Data and materials availability Videos of experiments are available through FigShare: https://figshare.com/s/1c65509f4e0e04afcde5.

Compliance with ethical standards

Conflict of interest The authors declare that they have no conflict of interest.

Ethical approval All applicable international, national, and/or institutional guidelines for the care and use of animals were followed.

References

Barbaglio A, Tricarico S, Di Benedetto C, Fassini D, Lima AP, Ribeiro AR, Ribeiro CC, Sugni M, Bonasoro F, Wilkie I, Barbosa M, Candia Carnevali MD (2013) The smart connective tissue of echinoderms: a materializing promise for biotech applications. Cah Biol Mar 54:713–720

Brainerd EL, Baier DB, Gatesy SM, Hedrick TL, Metzger KA, Gilbert SL, Crisco JJ (2010) X-ray reconstruction of moving morphology (XROMM): precision, accuracy, and applications in comparative biomechanics research. J Exp Zool 313A:262–279

Clark EG, Hutchinson JR, Darroch SAF, Mongiardino Koch N, Brady TR, Smith SA, Briggs DEG (2018a) Integrating morphology, skeletal mobility, and *in vivo* behavioral observations with digital models to infer function in brittle star arms. J Anat 233:696–714

Clark EG, Hutchinson JR, Darroch SAF, Mongiardino Koch N, Brady TR, Smith SA, Briggs DEG (2018b) Data from: Integrating morphology, skeletal mobility, and *in vivo* behavioral observations with digital models to infer function in brittle star arms. Project. (https://figshare.com/projects/Data_from_Integrating_morphology_and_in_vivo_skeletal_mobility_with_digital_models_to_infer_function_in_brittle_star_arms/37709

Ferrario C, Leggio L, Leone R, Di Benedetto C, Guidetti L, Coccè V, Ascagni M, Bonasoro F, La Porta CAM, Candia Carnevali MD, Sugni M (2017) Marine-derived collagen biomaterials from echinoderm connective tissue. Mar Environ Res 128:46–57

Fleming PA, Muller D, Bateman PW (2007) Leave it all behind: a taxonomic perspective of autotomy in invertebrates. Biol Rev Camb Philos Soc 82:481–510

Goh KL, Holmes DF (2017) Collagenous extracellular matrix biomaterials for tissue engineering: lessons from the common sea urchin tissue. Int J Mol Sci 18:901–949

Westneat MW, Betz O, Blob RW, Fezzaa K, Cooper WJ, Lee W-K (2003) Tracheal respiration in insects visualized with synchrotron X-ray imaging. Science 299:558–560

Wilkie IC (1978a) Arm autotomy in brittlestars (Echinodermata: Ophiuroidea). J Zool Lond 186:311–330

Wilkie IC (1978b) Functional morphology of the autotomy plane of the brittle star *Ophiocomina nigra* (Abildgaard) (Ophiuroidea, Echinodermata). Zoomorphologie 91:289–305

Wilkie IC (1978c) Nervously mediated change in the mechanical properties of a brittlestar ligament. Mar Behav Physiol 5:289–306

Wilkie IC (1984) Variable tensility in echinoderm collagenous tissues: a review. Mar Behav Physiol 11:1–34

Wilkie IC (1988) Design for disaster: the ophiuroid intervertebral ligament as a typical mutable collagenous structure. In: Burke RD, Mladenov PV, Lambert P, Parsley RL (eds) Echinoderm biology. AA Balkema, Rotterdam, pp 25–38

Wilkie IC (2001) Autotomy as a prelude to regeneration in echinoderms. Microsc Res Tech 55:369–396

Wilkie IC (2002) Is muscle involved in the mechanical adaptability of echinoderm mutable collagenous tissue? J Exp Biol 205:159–165

Wilkie IC (2005) Mutable collagenous tissue: overview and biotechnological perspective. In: Matranga V (ed) Echinodermata. Progress in molecular and subcellular biology (marine molecular biotechnology), vol 39. Springer, Berlin, pp 221–250

Wilkie IC, Emson RH (1987) The tendons of *Ophiocomina nigra* and their role in autotomy (Echinodermata, Ophiuroidea). Zoomorphology 107:33–44